JOURNAL OF MATERIALS SCIENCE 19 (1984) 2465–2472

Isothermal decomposition of the ß′ phase in a Cu–Zn–Al alloy

S. K. MANNAN, VAIDEHI GANESAN, M. VIJAYALAKSHMI, V. SEETHARAMAN
Materials Development Laboratory, Reactor Research Centre, Kalpakkam-603102, Tamilnadu, India

The isothermal decomposition of the β' phase in a Cu–25 wt % Zn–6 wt % Al alloy was investigated using transmission electron microscopy and electron probe microanalysis. The ordering of the β phase was too rapid to be suppressed during quenching from the solution annealing temperature. On ageing the alloy in the temperature range 603 to 703 K, the β' phase was found to decompose into a mixture of $\alpha + \gamma$ phases by the precipitation of fine and equiaxed γ-phase particles distributed uniformly throughout the matrix of α. The orientation relationship between α and γ was identified as

$$(0\,0\,1)_\alpha \| (0\,0\,1)_\gamma$$

$$[0\,1\,0]_\alpha \| [0\,1\,0]_\gamma$$

The growth rate of the γ phase precipitates exhibited a maximum at 653 K. Electron probe microanalysis showed that the γ phase precipitates were enriched in aluminimum and depleted in zinc, compared to the α matrix. In addition to the uniform distribution of intragranular γ phase precipitates, heterogeneous precipitation of the α phase was observed along the grain boundaries indicative of a direct transformation of β' to α in these regions: this reaction was found to be pronounced as the ageing temperature was increased up to 773 K.

1. Introduction

The β phase of Cu–Zn–Al alloys exhibits a variety of transformations including ordering [1], athermal martensitic transformation [2–7] and precipitation reactions [8]. While the ordering reaction, martensitic transformation and the associated shape memory effect [9–12] have been studied extensively, decomposition and precipitation reactions have received very limited attention [13]. Massalski and King [14] have shown that most of the noble metal based β phase alloys corresponding to an electron/atom ratio (e/a) of 1.5 become unstable at low temperatures with respect to the eutectoid decomposition, $\beta \rightarrow \alpha + \gamma$. However, this reaction is suppressed effectively, if the β phase undergoes ordering prior to decomposition. For example, the decomposition of β in binary Cu–Al alloys [15] occurs by a discontinuous precipitation only when the ordering of the β phase is avoided by rapid quenching of the alloys prior to isothermal ageing. On the other hand, in binary Cu–Zn alloys [14] the ordering of the β phase can not be prevented even by very rapid quenching and therefore the decomposition of β' in this alloy occurs by the homogeneous nucleation and growth of the γ phase.

This paper deals with the decomposition of β' in a ternary Cu–25 wt % Zn–6 wt % Al alloy. The morphological evolution of the γ phase precipitates has been followed using transmission electron microscopy and optical microscopy. The compositions of the different phases, namely α and γ, have been determined by electron probe microanalysis.

0022–2461/84 $03.00 + .12

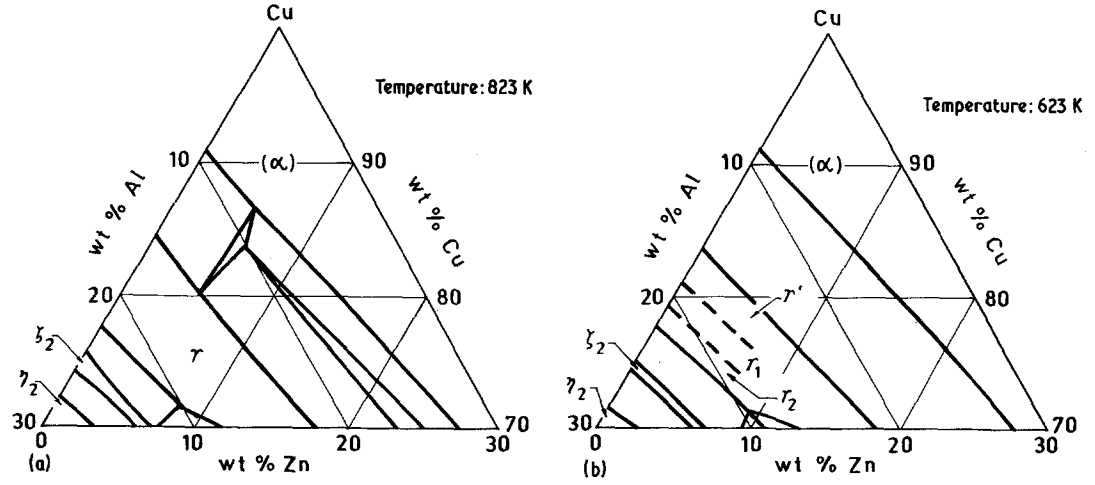

Figure 1 Isothermal sections of the Cu–Al–Zn phase diagram at 823 and 623 K [16].

2. Experimental procedure

An alloy of Cu–25 wt% Zn–6 wt% Al was induction melted in a graphite crucible using metals of high purity (better than 99.999%) and chill cast into cylindrical moulds. The ingots were homogenised at 1073 K for four days. Slices of 5 mm thickness were cut from these ingots and subjected to several cycles of cold work (20%) and annealing at 1073 K for 1 h. Electron probe microanalysis (EPMA) of these samples after the homogenization treatments showed that the concentrations of copper, zinc and aluminium were uniform both in macro and micro scales. These discs were subseqently cold pressed and hot rolled to yield strips of 0.15 mm thickness suitable for electron microscopy.

The sheets were solution annealed at 1073 K for 1 h followed by water quenching. Isothermal ageing treatments of the solution-annealed sheets were carried out in a resistance heated furnace for temperatures down to 603 K, while an oil bath was used for ageing at 473 K. All the ageing treatments were followed by water quenching. Metallographic specimens were etched with Vilella's reagent (1 g picric acid 5 ml HCl and 100 ml CH_3OH) to reveal the microstructure both for optical microscopy and EPMA. The Cameca MS 46R electron microprobe was used for this work and all the microanalyses were carried out at an acceleration voltage of 20 kV and at a specimen current of 80 nA. The X-ray intensity ratios obtained in EPMA were converted into true composition data using the ZAF correction procedure [17, 18]. Thin foils for transmission electron microscopy (TEM) were prepared by electrolytic polishing in a solution containing 25 g of anhydrous Cr_2O_3, 133 cc of acetic acid and 7 cc of water at 283 K and at a voltage of 10 V. The foils were examined in a Philips EM 400 TEM operated at 120 kV.

3. Results and discussions

On the basis of the isothermal sections of the Cu–Zn–Al ternary phase diagram [16] shown in Fig. 1, the following phase transformations are expected for the alloy under investigation

$$\beta \rightarrow \beta' \quad \text{at } T \leqslant T_c$$

$$\beta' \rightarrow \alpha + \beta' \text{ at } T = 823 \text{ K}$$

$$\beta' \rightarrow \alpha + \gamma \text{ at } T = 623 \text{ K}$$

where T_c is the critical temperature for ordering. At intermediate temperatures (623 to 823 K), the alloy is expected to remain within the three phase field of α, β and γ shown as the tie triangle in Fig. 1a and b.

3.1. Transmission electron microscopy

The present study is confined to the precipitation of $\alpha + \gamma$ from β phase. The morphological evolution of the γ phase was studied in detail using TEM. The microstructure of the sample solution annealed at 1073 K followed by water quenching contained only the matrix. The presence of {1 0 0}-type super lattice spots in the selected area diffraction pattern shown in Fig. 2 confirms that the β matrix has transformed to the ordered β' phases. It is found that the lattice parameter of the β' phase is 0.294 nm which compares well

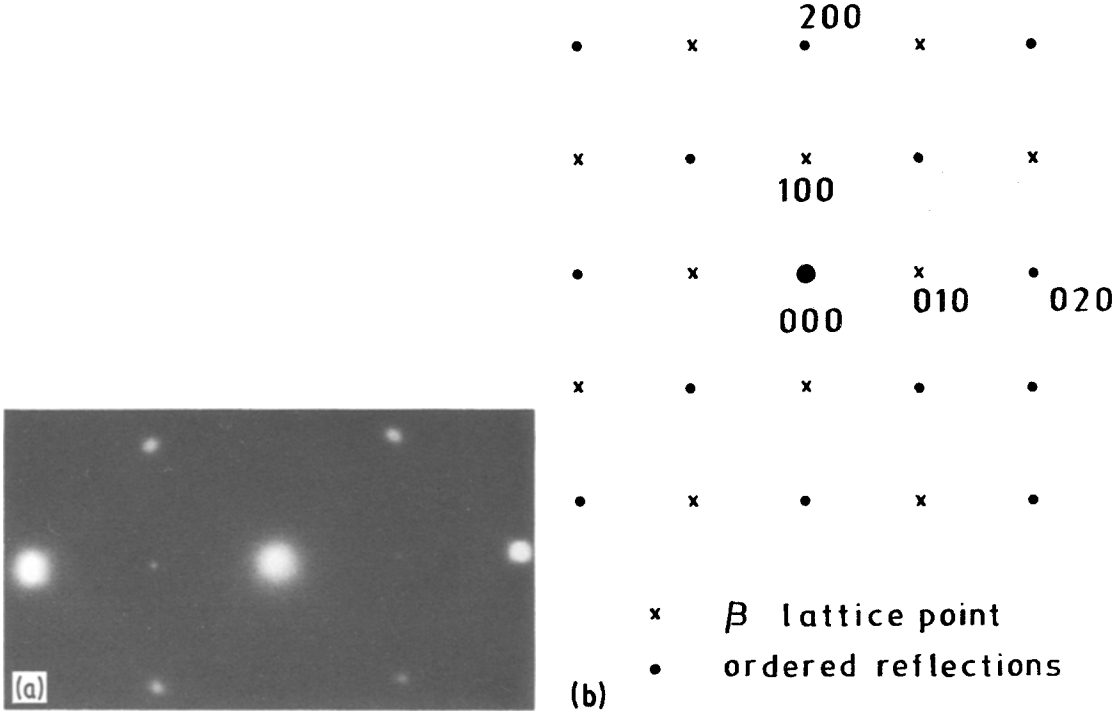

Figure 2 (a) Selected area diffraction pattern taken from the solution annealed and quenched specimen. (b) Key for the SAD pattern shown in (a) illustrating the (0 0 1) reciprocal lattice section of the β' phase.

with the value of 0.295 nm reported for the binary Cu–Zn system.

On ageing the β' matrix at 473 K for 1 h, extremely fine precipitates of ~ 10 nm diameter were observed. Continuation of ageing up to 3 h led to the formation of uniformly distributed spherical particles of about 20 nm diameter (Fig. 3).

By allowing the reaction $\beta' \rightarrow \alpha + \gamma$ to proceed at a higher ageing temperature of 603 K for fifteen minutes, quite coarse particles of 0.2 μm diameter were found to be uniformly distributed in the matrix (Fig. 4). The precipitates are more clearly visible in the dark field (Fig. 4b) than in the bright field. The growth rate of these precipitates was quite rapid at this temperature leading to the formation of 1.2 μm diameter particles after 16 h of ageing as seen in Fig. 5. It is observed that the precipitates retain their spherical morphology from the early stages of precipitation till these coarsen to fairly large size. It was also noticed that the coalescence of these precipitates occurred at a later stage of coarsening. The identification of the precipitates was carried out by analysing the selected area diffraction pattern taken from the precipitate alone. Fig. 5b shows the (0 0 1) zone of a cubic crystal from which the lattice parameter of the precipitates is estimated as 0.87 nm. Hence, these spherical precipitates have been identified as ordered cubic γ phase with $a = 0.87$ nm which is in agreement with the $D8_2$ structure of the γ phase reported by Bradley and Gregory [19]. This value of lattice parameter is comparable to the value of $a = 0.886$ nm reported for the Cu–Zn system.

The growth of these γ phase particles at 703 K was found to be more rapid than that at 603 K. However, the maximum growth rate of the γ precipitates was observed at 653 K. It should be mentioned in this context, that on ageing at 703 K, the γ phase precipitates remained as isolated spherical particles even after considerable growth (Fig. 6a). On the other hand, ageing at 653 K caused coalescence of the individual particles leading to the type of microstructure illustrated in Fig. 6b.

The lattice parameter of the α phase has been estimated as 0.294 nm from the analysis of electron diffraction patterns. It can be seen that the lattice parameter of γ is approximately three times that of the α matrix and this should, therefore, lead to good matching across the two lattices.

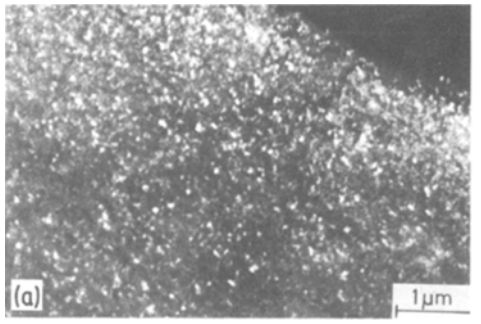

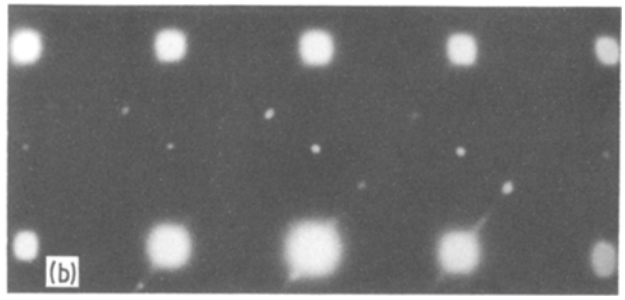

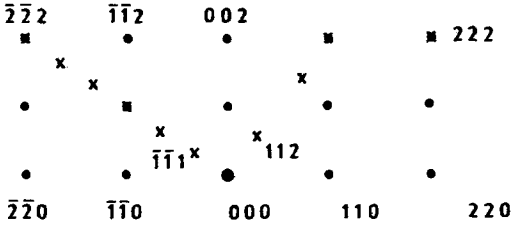

(c) • β × γ

Figure 3 (a) Transmission electron micrograph of the sample quenched and aged at 473 K for 3 h showing a high density of the γ phase precipitates. (b) The diffraction pattern showing the superimposed reciprocal lattice sections of the β′ and the γ phases. (c) Key for the diffraction pattern. It is clear that the β′ and γ phases exhibit cube–cube orientation relationship.

The orientation relationship between the α matrix and the γ phase precipitates has been established by analysing the superimposed diffraction patterns shown in Fig. 7.

$$(0\,0\,1)_\alpha \| (0\,0\,1)_\gamma$$

$$[0\,1\,0]_\alpha \| [0\,1\,0]_\gamma$$

It is clear that the high degree of coherency between the α/γ phases is responsible for the retention of the spherical morphology of the γ phase even after considerable growth.

3.1.1. Growth kinetics of the γ phase

The growth of the γ phase at 603, 653 and 703 K was followed by measuring the mean size of the γ phase particles as a function of the ageing time at these temperatures. Fig. 8 shows the linear dependence of the mean diameter, $\bar{D}$ on the cube root of the ageing time. This suggests that the growth of the γ phase is dominated by a volume diffusion controlled process. The growth rates were measured from the slopes of these plots (full lines) as 0.032, 0.12 and 0.027 μm $sec^{-1/3}$ at 603, 653 and 703 K, respectively. It is clear that the temperature dependence of the growth rate shows a C-curve behaviour with its maximum at 653 K indicating that the activation energy for the growth process is temperature dependent. These data on the growth kinetics of γ phase precipitates obtained by transmission electron microscopy were found to be consistent with the electrical resistivity measurements [20].

The dotted lines shown in Fig. 8 correspond to the extrapolation of the growth kinetics to zero ageing time. The slopes of these lines suggest that

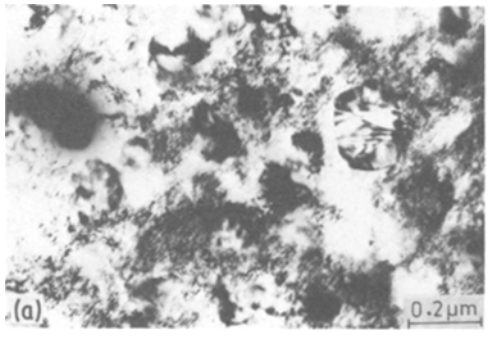

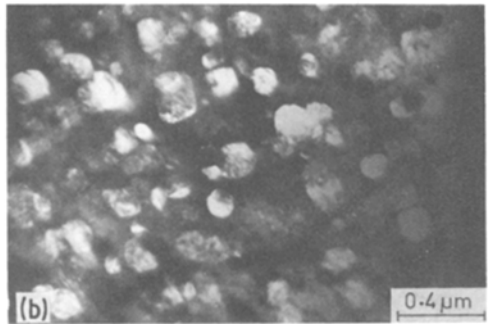

Figure 4 Microstructures of the sample aged at 603 K for 900 sec showing the γ phase precipitates of about 0.2 μm diameter distributed uniformly within the α matrix. (a) Bright field; (b) dark field.

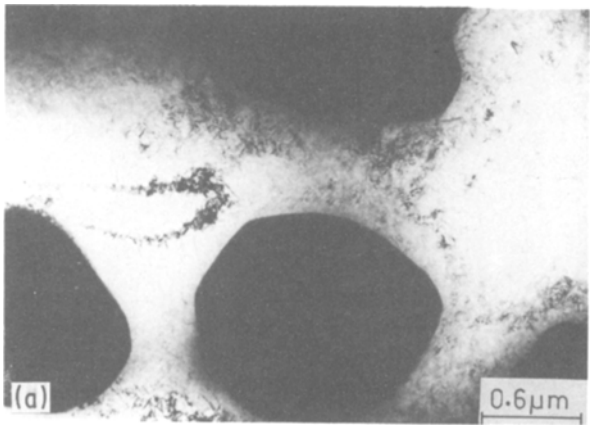

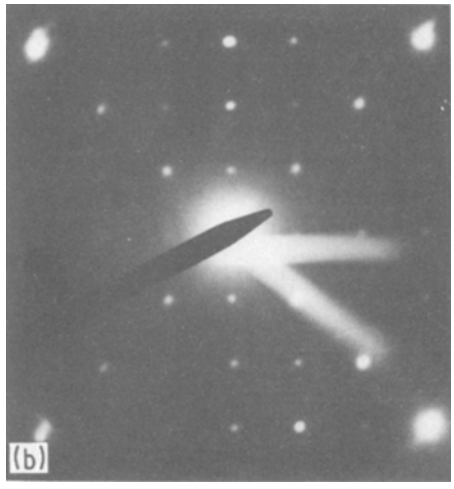

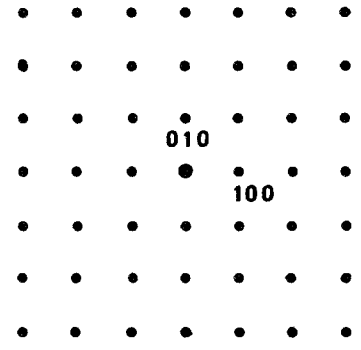

(c)

Figure 5 (a) Coarsening of the γ phase particles during ageing at 603 K for 16 h; (b) selected area diffraction pattern taken from the precipitates; (c) key.

the growth rates of the γ phase at 603 and 653 K in the initial stages are smaller than those corresponding to the later stage. The changes in growth rate can be attributed to the partial loss of coherency between α and γ at the end of initial stage. In this context, it is interesting to consider the observations made by Rastogi and Ardell [21]. They have shown that the growth rate of the γ' precipitates in Ni–Si alloys is enhanced due to the breakdown in the coherency between the matrix and γ'.

3.2. Optical microscopy

In order to determine the highest temperature at which $\alpha + \gamma$ phase field is stable, long term ageing treatments were carried out at 603 K for 16 h and at 733 and 773 K for 5 h. It was seen that in addition to the spherical precipitates of the γ phase distributed uniformly throughout the matrix, another kind of precipitate was found exclusively along the grain boundaries. The grain boundary precipitation becomes pronounced as the ageing temperature is increased. It is also interesting to note the presence of a narrow precipitate free zone of $\sim 5\ \mu$m width adjacent to the grain boundary (Fig. 9). Similar grain

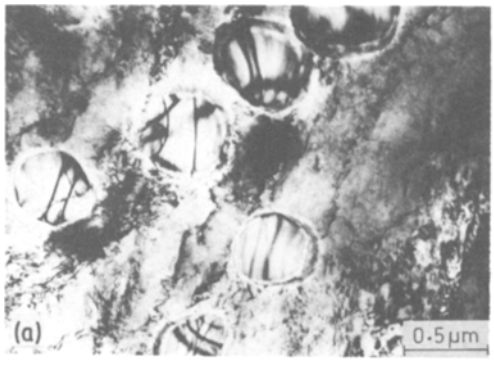

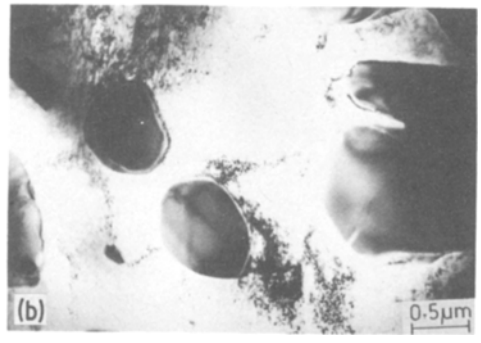

Figure 6 (a) Coarsening of the individual precipitates on ageing at 703 K for 10 min. (b) Coalescence of the γ phase particles during ageing at 653 K for 90 min.

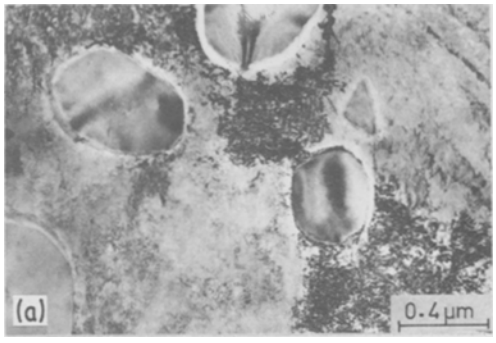

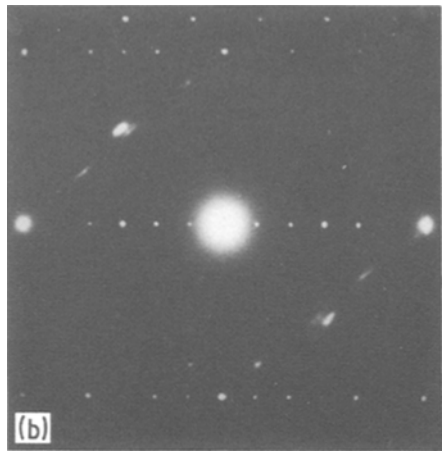

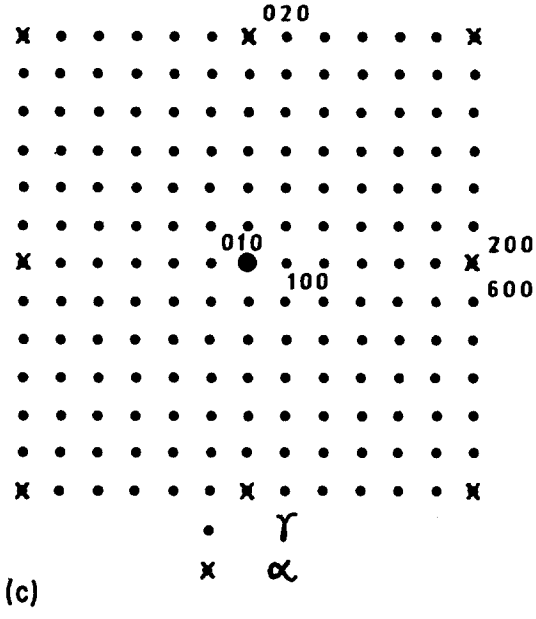

Figure 7 Transmission electron micrographs obtained on ageing at 703 K for 1 h. (a) Bright field; (b) selected area diffraction pattern showing the superimposed reciprocal lattice sections of the α and the γ phase and; (c) key.

boundary allotriomorphs have been encountered by several investigators [22–24] in Cu–Zn binary alloys and have been identified as the product of the reaction $\beta(\beta') \rightarrow \alpha$. Therefore, it is reasonable to conclude that the grain boundary phase observed in Fig. 9 corresponds to the α phase, but produced as a result of the direct transformation of β' to α.

The decomposition of $\beta' \rightarrow \alpha + \gamma$ could have taken place through two different mechanisms, i.e.

$$\beta' \rightarrow \alpha \rightarrow \alpha + \gamma$$

or

$$\beta' \rightarrow \alpha + \gamma$$

In the present work, there was no evidence for the operation of the former reaction mechanisms, except along the grain boundaries. Therefore the direct decomposition of β' into a mixture $\alpha + \gamma$ is the main operative mechanism. It should also be mentioned that no transition phases were observed right from the initial stage of decomposition. However, the exact mechanism associated with the nucleation of γ is not very clear.

3.3. Electroprobe microanalysis

Detailed electron probe microanalysis was carried out to determine the composition of various type

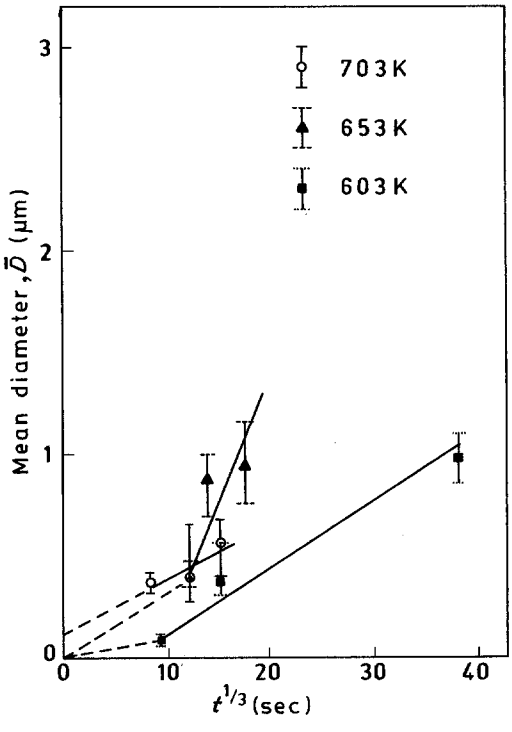

Figure 8 Growth kinetics of the γ phase precipitates in the matrix.

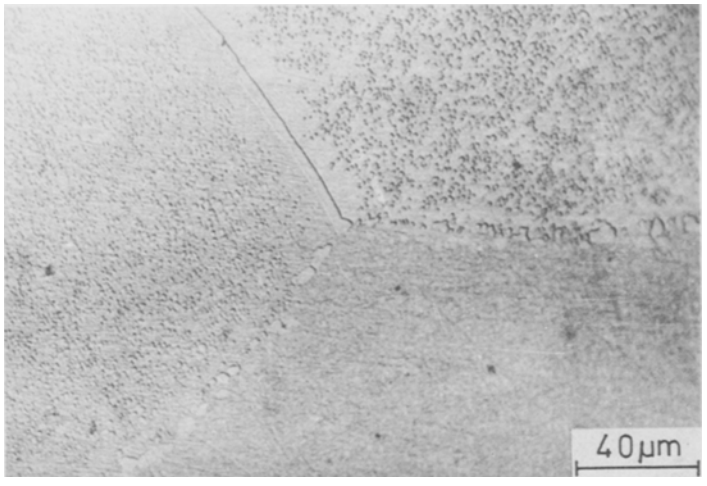

Figure 9 Optical micrograph of the sample aged at 773 K for 5 h. Extensive precipitation along the grain boundaries and the presence of a precipitate free zone in the adjacent regions are evident.

of precipitates. The size of spherical γ phase precipitates was only of the order of 1 to 2 μm, even after 16 h of ageing at 603 K. This was too small to permit accurate and unambiguous analysis of the γ phase. Hence, microanalysis of the γ phase was carried out in samples aged at 703 K for 3 h, in which the mean diameter of γ phase particles was 5 μm. The results of the microanalysis are shown in Table I. All the compositions listed in Table I represent the average of the data collected from ten such precipitate particles. It was found that the intragranular γ phase particles were enriched in aluminium and depleted in zinc compared to the matrix. Similar analysis was carried out for the grain boundary precipitates observed after ageing at 773 and 733 K. It is found that the grain boundary precipitates are also enriched in aluminium and depleted in zinc, but the extent of enrichment of aluminium in the grain boundary precipitates is more than that of the intragranular γ phase precipitates (Table I). Microanalysis of the samples aged at 733 and 773 K revealed that (a) the precipitated free zone adjacent to the grain boundary (Fig. 9) had nearly the same composition as that of the α matrix and (b) the grain boundary precipitates were found to contain more zinc and aluminium compared to that of matrix precipitates. The compositional differences between these regions is expected to be within 10% from the phase diagram consideration. Hence, the microanalysis results should be considered as merely indicative of the trend of solute redistribution.

TABLE I Chemical composition of the different constituents determined by electron probe microanalysis

Sample	Ageing temperature (K)	Ageing time (h)	Region of microanalysis	Concentration (wt %)*		
				Cu	Zn	Al
1	703	3	Matrix	66.24 ± 0.78	27.04 ± 0.53	6.72 ± 0.48
			Intragranular precipitates	67.57 ± 0.81	21.98 ± 1.19	10.45 ± 0.84
2	733	5	Matrix	67.37 ± 0.44	25.87 ± 0.38	6.76 ± 0.44
			Grain boundary precipitates	67.83 ± 0.53	22.94 ± 0.64	9.23 ± 0.34
			Matrix	68.06 ± 0.61	26.71 ± 0.56	5.23 ± 0.63
			Intragranular precipitates	70.61 ± 0.82	20.57 ± 0.54	8.82 ± 0.92
3	773	5	Grain boundary phase	69.80 ± 0.44	21.18 ± 0.67	9.02 ± 0.53
			Precipitate free zone	67.41 ± 0.38	27.41 ± 0.26	5.18 ± 0.51

*The error bounds correspond to the 2-sigma limits

4. Conclusions

Isothermal phase transformation in a β' Cu–Zn–Al alloy have been studied using transmission electron microscopy and electron probe microanalysis. The main conclusions of this study are:

(a) In the temperature range 603–703 K, the ordered phase, β', decomposed into a mixture of $\alpha + \gamma$ by the uniform precipitation of spherical γ phase particles in a matrix of α. The maximum growth rate of the γ phase precipitates was found at 653 K.

(b) The γ phase was found to retain spherical morphology even after substantial coarsening.

(c) The orientation relationship between the α and γ phases was found to be

$$(0\,0\,1)_\alpha \| (0\,0\,1)_\gamma$$

$$[0\,1\,0]_\alpha \| [0\,1\,0]_\gamma$$

(d) The γ phase precipitates were found to be richer in aluminium and leaner in zinc than the α phase.

Acknowledgements

The authors would like to thank Dr P. Rodriguez, Head, Metallurgy Programme for his constant encouragement during the course of this work. The authors are also grateful to Messrs S. Venkadesan and S. Venugopal for their help in the preparation of this alloy.

References

1. R. D. GARWOOD, *J. Inst. Met.* 83 (1954) 64.
2. F. C. LEFEVER, M. CHANDRASEKARAN, R. RAPACIOLI and M. AHLERS, *Z. Metall.* 71 (1981) 37.
3. F. C. LEFEVER, M. CHANDRASEKARAN and M. AHLERS, *ibid.* 71 (1981) 43.
4. W. DEJONGHE, R. DEBATIST, L. DELAEY and M. DEBONTE, in "Shape Memory effects in alloys" edited by Jeff Perkins (Plenum Press, New York, 1975) p. 451.
5. I. CORNELIS and C. M. WAYMAN, *Acta Metall.* 22 (1974) 294.
6. H. POPS, *Met. Trans.* A6 (1975) 251.
7. D. P. DUNNE and N. F. KENNON, *Scripta Metall.* 16 (1982) 729.
8. H. HANEMANN and A. SCHRADER, in "Ternare Legierungen des Aluminium Atlas Metallographicus", Vol. III (Verlag Stahleisen gMBH, Dusseldorf, 1952) p. 94.
9. S. VATANAYON and R. F. HEHEMANN, in "Shape Memory Effects in Alloys" edited by Jeff Perkins (Plenum Press, New York, 1975) p. 115.
10. R. RAPACIOLI, M. CHANDRASEKARAN and L. DELAEY, in "Shape Memory Effects in Alloys" edited by Jeff Perkins (Plenum Press, New York, 1975) p. 365.
11. M. AHLERS, R. RAPACIOLI and W. ARNENDO, *ibid.* 379.
12. R. RAPACIOLI, M. CHANDRASEKARAN, M. AHLERS and L. DELAY, *ibid.* p. 385.
13. N. F. KENNON, D. P. DUNNE and L. MIDDLETON, *Met. Trans.* A16 (1982) 551.
14. T. B. MASSALSKI and H. W. KING, in "Progress in Materials Science", Vol. 10, edited by B. Chalmers (Pergamon Press, London, 1961) p. 1.
15. K. KURIBAYASHI, S. TANIGAWA, S. NANAO and M. DAYAMA, *Scripta Metall.* 8 (1975) 423.
16. TAYLOR LYMAN (ed.) "Metals Handbook", Vol. 8. (American Society of Metals, Metals Park, Ohio, 1975).
17. J. COLBY, "Advances in X-ray Analysis" (Plenum Press, New York, 1968) p. 287.
18. D. R. DEAMAN and J. A. ISASI, *Anal. Chem.* 42 (1970) 1540.
19. A. J. BRADLEY and C. H. GREGORY, *Phil. Mag.* 12 (1981) 143.
20. S. K. MANNAN, M. VIJAYALAKSHMI, V. SEETHARAMAN and V. S. RAGHUNATHAN: Reactor Research Centre, Kalpakkam, India (1983) unpublished research.
21. P. K. RASTOGI and A. J. ARDELL, *Acta Metall.* 19 (1971) 321.
22. G. W. LORIMER, G. CLIFF, H. I. AARONSON and K. R. KINSMAN, *Scripta Metall.* 9 (1975) 271.
23. E. HORNBOGEN and H. WARLIMONT, *Acta Metall.* 15 (1967) 942.
24. P. E. J. FLEWITT and J. M. TOWNER, *ibid.* 14 (1966) 1013.

Received 21 March
and accepted 21 September 1983